Polypropylene during Crystallization from the Melt as a Model for the Rheology of Molten-Filled Polymers

KHALED BOUTAHAR, CHRISTIAN CARROT,* and JACQUES GUILLET

Laboratoire de Rhéologie des Matières Plastiques, Faculté de sciences et Techniques, Université Jean Monnet, 23, Rue du Docteur Paul Michelon, 42023 Saint-Etienne, Cedex 2, France

SYNOPSIS

Polarized light microscopy shows that polypropylene crystallizes from the melt into a well-distinguished spherulitic structure. Therefore, it provides a useful model for molten-filled polymers, where the growing spherulites are considered to be filler particles dispersed in a matrix fluid. Although spherulites are randomly dispersed in the space, two dispersion models (simple cubic and centered cubic) are discussed to correlate the transformed fraction $\alpha(t)$ with the volume fraction of filler $\phi(t)$. The combination of these results with those of differential scanning calorimetry (DSC) shows that the transformed fraction $\alpha(t)$ is a direct indication of the volume fraction of filler $\phi(t)$. The rheological study, using oscillatory experiments coupled with DSC results, shows the relative sensitivity of the rheological functions to structural changes of the liquid during crystallization. Furthermore, they reveal the existence of a yield effect above a certain critical value of the filler content ($\phi_c = 0.4$). In the absence of this yield effect, a model is proposed to predict the variation of the rheological functions with the filler content. This model shows not only a variation of the plateau modulus, but also the modification of the characteristic times of relaxation of the polymer matrix, whereas the shape of the relaxation spectrum remains unchanged. © 1996 John Wiley & Sons, Inc.

INTRODUCTION

Rheological Behavior

The rheological behavior of filled polymers strongly depends on a large number of parameters such as volume fraction, shape and size of particles, filler–filler and filler–matrix interactions. The influence of the volume fraction on the main flow functions such as viscosity and normal stress coefficients has been the most extensively discussed in the literature.[1-3] In order to overcome problems arising from the shape or anisometry of the particles, several authors[1,5-10] have used spherical particles such as glass beads and metal spheres. In general, the models proposed are concerning the steady shear flow. They are derived from theories established for suspensions of elastic particles in a Newtonian fluid. However, little attention has been paid to dynamic rheological properties in the melt, and the few equations proposed in this field are, in fact, empirical extensions of the steady shear flow models. The use of the relative dynamic viscosity in the classical theories has been introduced by Faulkner and Schmidt.[11] Poslinski et al.[12] have extended this work and proposed an empirical equation for the relative storage modulus. The continuum mechanics approach has been first used by Kerner[13] and Takayanagi et al.[14] Dickie,[15] Dickie et al.,[16] and, more recently, Palierne[17] have used this approach to get expressions for the dynamic modulus of spherical dispersed phases in polymer blends. None of these equations takes into account changes of the relaxation time distribution or time spectrum upon addition of the filler, because, for example, with Palierne's model for rigid fillers the relative dependence of both the storage and loss moduli vs. volume fraction is predicted to be the same. Nor are these equations able to take into account the occurrence of yield stress.

* To whom correspondence should be addressed.

Journal of Applied Polymer Science, Vol. 60, 103–114 (1996)
 CCC 0021-8995/96/010103-12

One feature of highly filled polymers is the existence of a yield stress. It is defined as the value of the stress above which there is flow. Below this value the material behaves like a solid. Casson[18] proposed an equation for flow curves in which he took into account the existence of yield stress:

$$\tau^{1/2} = Y^{1/2} + a\,\dot{\gamma}^{1/2} \tag{1}$$

where Y represents the yield stress and $a\gamma^{1/2}$ the matrix contribution. This equation has been extended by Utracki,[19] who replaced the shear stress by any rheological function F and the shear rate by F_0, which represent the value of F for the pure matrix liquid at the same shear rate or frequency. Due to the analogy between the shear stress τ and the components of the complex modulus G^*, we may expect that the modified Casson equation might be a useful means to calculate the yield values of the real and the imaginary parts G' and G'' of the complex modulus G^*.

Leonov[20] has proposed another approach wherein he described the rheological behavior of filled polymers by a model in which the total mean stress τ is represented by the following sum:

$$\tau = \tau_m + \tau_p \tag{2}$$

where τ_m represents the mean stress arising in a suspension of inactive particles in a matrix, and τ_p is an additional mean stress due to the particle-to-particle interactions in the particulate phase. The matrix mode was described using viscoelastic equations known for pure polymers (Maxwellian modes). In this description, the dependencies of the rheological parameters on the particle loading ϕ was included. For the particle mode, he took into account both the effect of finite elasticity and the dissipative effect. Therefore, assuming that the matrix parameters are independent of the particle size, only hydrodynamic interactions between particles of filler are assumed to have an effect on the behavior of the polymer matrix. Leonov[20] used the following equations in the case of a simple Maxwell model:

$$\frac{\eta_0(T, \phi)}{\eta_0(T, 0)} = \frac{G_0(T, \phi)}{G_0(T, 0)} = \left(1 - \frac{\phi}{\phi_M}\right)^{-2} \tag{3}$$

where, $\eta_0(T,0)$ and $G_0(T,0)$ are, respectively, the Newtonian viscosity and the plateau modulus of the pure matrix at temperature T, and ϕ_M is the maximum packing volume. From this, it can be deduced that:

$$\lambda_0(T, \phi) = \frac{\eta_0(T, \phi)}{G_0(T, \phi)} = \frac{\eta_0(T, 0)}{G_0(T, 0)} = \lambda_0(T, 0) \tag{4}$$

It means that the relaxation times in the filled polymer matrix remains the same as for the case of pure polymers. Furthermore, he suggested that the above equation may be applied to the multimodal representation of the rheological behavior of the polymeric matrix where all the relaxation times in the matrix mode are also assumed to be independent on the filler loading and size. Poslinski et al.[12] have proposed a model derived from the Bird–Carreau equation to determine the suspension viscosity $\eta(\dot{\gamma},\phi)$, taking into account the existence of the yield stress:

$$\eta(\dot{\gamma}, \phi) = \tau_y(\phi)\dot{\gamma}^{-1} + \eta_0(\phi)[1 + (\lambda_0(\phi)\dot{\gamma})^2]^{(n-1)/2} \tag{5}$$

τ_y is the yield stress that increases with the addition of particulates. $\dot{\gamma}$ is the shear rate, and n the power law index of the matrix polymer. Poslinski et al.[12] stated that both the Newtonian viscosity and the characteristic relaxation time λ_0 are functions of the volume fraction of filler ϕ. They proposed the following equations to describe them:

$$\eta_0(\phi) = \eta_0(0)\left(1 - \frac{\phi}{\phi_M}\right)^{-2} \tag{6}$$

$$\lambda_0(\phi) = \lambda_0(0)\left(1 - \frac{\phi}{\phi_M}\right)^{-2} \tag{7}$$

Utracki[21] also showed that the filler modifies the characteristic time of relaxation and used the following relation, which describes the $\lambda_0(\phi)$ dependence:

$$\lambda_0(\phi) = \lambda_0(1 - \phi)^{-n}3 \tag{8}$$

where n_3 is an empirical constant.

Although the expressions proposed are not similar, Poslinski et al.[12] are in accordance with Utracki[21] on the fact that the characteristic times of relaxation are dependent on the filler content ϕ. However, this is in contradiction with Leonov's[20] approach, which states that the relaxation times are not a function of the particle loading. This is also the point of view of continuum mechanics approaches.[13–17] One of the aims of this work is mainly to get a deeper insight and to clarify this dependence of the relaxation spectrum on the volume fraction. In a previous work[22] we proposed a new approach to check the validity of the various laws relating

dynamic rheological parameters to the volume fraction of filler. This approach considers that during isothermal crystallization a molten and crystallizing polymer provides a useful model for filled polymers. In the initial stage, the molten polymer can be considered as a homogeneous liquid. During the subsequent crystallization, a crystalline solid phase appears and smoothly grows in the continuous medium until the maximum crystallinity is achieved. The growing spherulites can be roughly considered to form a high modulus spherical phase dispersed in the remaining liquid matrix. The amorphous phase linking liquid and spherulites provides perfect adhesion between both matrix and filler. Furthermore, concentration gradients of the filler hardly occur because the crystalline nuclei appear randomly throughout the entire matrix. It should be noted that more recently Teh et al.[23] have used this type of experiment for crystallizing polyethylene, polypropylene, and their blends. Their goal was mainly to detect the onset of nucleation and to deduce semiquantitative data on the nucleation density and the initial crystallization rate. In the present work, we use polypropylene crystallizing from the melt as a model for dispersion of spherical rigid spheres in a molten matrix. Indeed, under proper conditions, polypropylene crystallizes isothermally in spherulitic structure, which, from the rheological point of view, may act as a rigid filler in a liquid. Crystallization, being a continuous process, can be followed in a rheometer. Thus, this provides a very useful model system for any study of the variation of the rheological functions towards volume fraction of filler, because the latter is obviously increasing during the process. However, in order to find proper conditions, we discuss hereafter some considerations about crystallization of polypropylene.

Crystallization of Polypropylene from the Melt

Polypropylene has mainly four different crystalline structures. The α-structure has been determined by Natta and Corradini[24] to be a monoclinic structure and it is obtained by crystallization either from the melt or in solution. Norton and Keller[25] attributed the apparition of the second structure or β-hexagonal structure to different factors among them, the presence of a nucleating agent or a rapid cooling or also shearing at the melt state. Turner–Jones et al.[26] have identified a third structure named triclinic γ-phase. This structure is obtained from the melt under elevated pressure. The fourth structure or δ-phase is obtained during quenching at very low temperatures. It has to be noticed that under particular conditions, structures β, γ, and δ may be transformed into the α-structure, which is known to be the most stable phase. Thus, Morrow[27] shows that the β-phase can be transformed into the α-phase by a recrystallization mecanism from the melt at higher crystallization temperatures. Similarly, the γ-phase may be transformed into the α-phase if it is heated and then cooled at lower rates to allow a recrystallization.

In general, once polypropylene is crystallized from the melt, a spherulitic structure is obtained. Spherulites are generally formed with radial lamellae, which grow from central nuclei. In their work on the crystallization of polypropylene using thin films at a range of temperature of 110 to 148°C, Padden and Keith[28] have identified four different types of spherulites, types I to IV. The formation of one type or another depends strongly on the crystallization temperature. Their classification depends on both the nature of the crystalline structure and the value and the sign of the birefringence. The work of Padden and Keith,[28] confirmed also by the work of Norton and Keller,[25] stated that types I and II crystallize into an α-monoclinic structure with a low absolute value of the birefringence but with different sign (positive for type I and negative for type II). This difference in the sign is attributed to the fact that type I contains more tangential lamellae than type II. Types III and IV crystallize into a β-structure with radial lamellae and a high negative birefringence. In their study on the crystallization of polypropylene at 135, 140, and 145°C, Norton and Keller[25] obtained an α-structure spherulites and show that the rate of tangential lamellae decreases with increasing the crystallization temperature and is almost zero at 145°C. However, Idrissi et al.[29] have found that the rate of tangential lamellae is equal to zero at 155°C. They explained that by the fact that tangential lamellae are less thick than the radial ones and, therefore, melt before them. Two other lamellar morphologies called quadrites and axialites were identified. Quadrites or "crosshatch type lamellar branching" appear in all the α-type spherulites. They were shown to be networks of two parallel sets of lamellae, crossing each other at an angle of about 80° proposed by Khoury.[30] Vaughan and Basset[31] show that the axialite structure has been identified into several systems and under particular crystallization conditions. This type of structure appears when the nucleation density is high and the volume offered for the growth is so limited that the spherulites cannot grow. This morphology is favored when the crystallization temperature approaches the melting point. In the case of polypropylene, this

structure is identified at a crystallization temperature near 160°C.

In order to get a spherulitic structure, the previous considerations led us to make experiments at relatively low temperature. From this, we can now try to check the validity of a model system for the rheological behavior of filled polymer by combining results obtained from differential scanning calorimetry, polarized light microscopy, and dynamic oscillatory experiments. And further, we will try to establish a model to predict the variation of the rheological parameters with the filler content.

EXPERIMENTAL

Material

Experiments were carried out using a commercial polypropylene (M_w = 300 000 g/mol, polydispersity index = 0.7). This polymer was found to be suitable for this study because it crystallizes from the melt into a well distinguished spherulitic structure, and for which it is easy to follow the evolution of the spherulite dimensions with time. Isothermal crystallizations were performed at 135°C. At this crystallization temperature, polypropylene crystallizes into an α-structure, which is the most stable phase. Furthermore, this temperature is sufficently high to avoid a very rapid crystallization, and consequently allows an easier following of the evolution of the spherulite dimensions. Moreover, it is far enough from the melting point to avoid the formation of the axialites and to insure that only spherulites are formed.

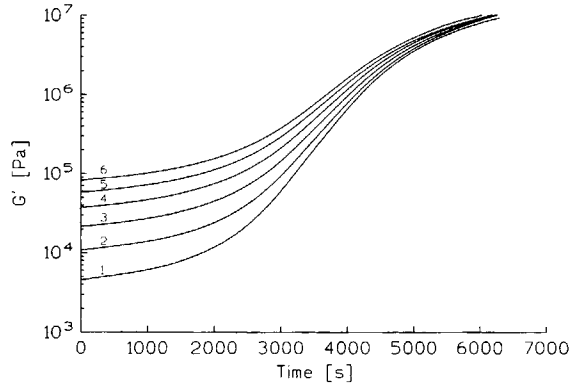

Figure 1 Evolution of the storage modulus during the crystallization at 135°C. Frequency: (1) ω = 0.3162 rad/s; (2) ω = 1 rad/s; (3) ω = 3.162 rad/s; (4) ω = 10 rad/s; (5) ω = 31.62 rad/s; (6) ω = 100 rad/s.

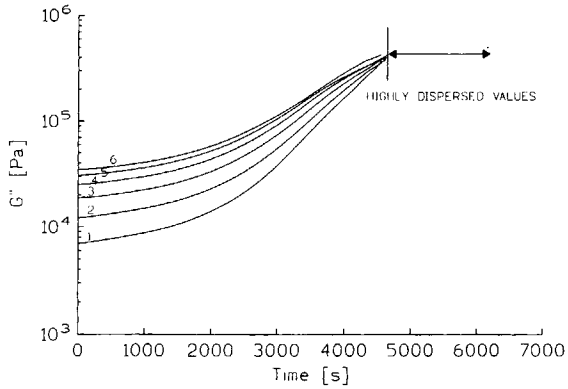

Figure 2 Evolution of the loss modulus during the crystallization at 135°C. Frequency: (1) ω = 0.3162 rad/s; (2) ω = 1 rad/s; (3) ω = 3.162 rad/s; (4) ω = 10 rad/s; (5) ω 31.62 rad/s; (6) ω = 100 rad/s.

Rheometry

Rheological oscillatory experiments were performed during isothermal crystallization at 135°C in a Rheometrics RDA 700 rheometer with a parallel plate geometry (plate diameter = 25 mm). The samples were injection-molded discs with 2 mm in thickness and 25 mm in diameter. Six frequencies were used (0.3162, 1, 3.162, 10, 31.62, and 100 rad/s) and the measurements were performed at equal time intervals during crystallization. Special care have to be taken concerning the following points.

Temperature Control

The temperature is measured on the upper plate of the rheometer. At first, the polypropylene sample is maintained for 5 min at its thermodynamic melting point, 210°C. This enables the complete melting of crystallites in the sample. The temperature is then lowered until the choosen crystallization temperature. This is done in a time interval of about 10.8 min. During the isothermal crystallization, the temperature fluctuation did not exceed ± 0.2°C.

Strain Amplitude Control and Gap Adjustment

During the crystallization, some precautions have to be taken to avoid the process being influenced by the operating conditions.

The strain must be small enough to avoid any disturbance in the crystallization kinetics and to insure that any parameter is only time and temperature dependent and not strain dependent. This is difficult to achieve with systems that change during the experiment. To take this into account, the strain has been adjusted during the test to get a low torque level compatible with the transducer sensitivity.

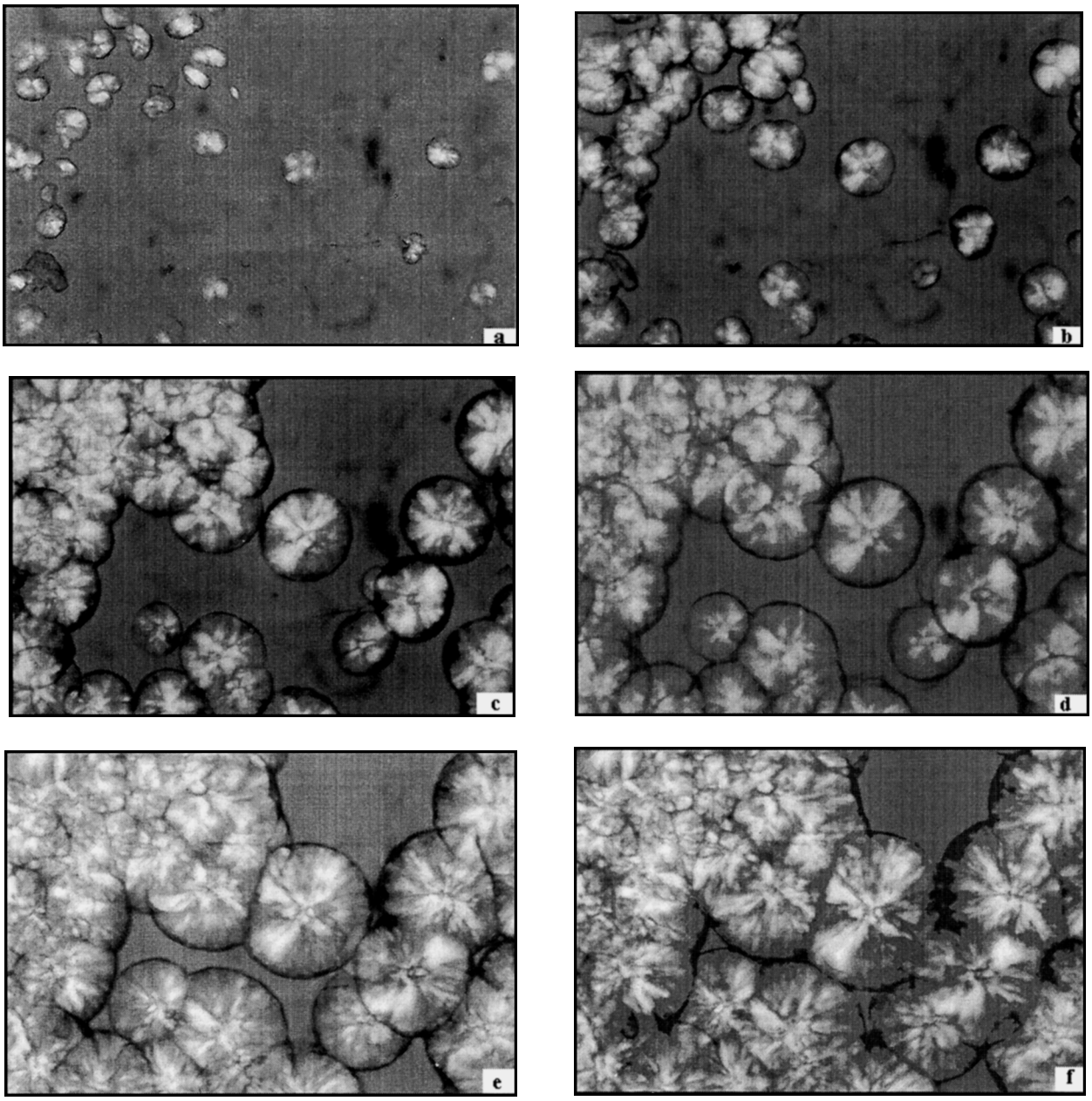

Figure 3 Polarized light microscopy photographs of polypropylene sample crystallized from the melt at T_c = 135°C taken at different time intervals. (a) t = 11.43 min; (b) t = 18.06 min; (c) t = 27.78 min; (d) t = 33.77 min; (e) t = 42.38 min; (f) t = 50.78 min.

The dimensional changes of the sample during the crystallization may induce an important error on the measured values that have to be corrected. Indeed, these uncontrolled dimensional changes would have two main effects: on one hand, the sample would be subjected to a tensile stress. On the other hand, the effective radius would be lower than the initial one and decreases with time. It is found that the error made in this case is as large as 25%. In a previous article[22] a detailed method was proposed to escape from these disagreements and to get the corrected values of the rheological parameters. It has been found to be better to adjust the gap throughout the test, according to the tensile force transducer of the rheometer, in order to keep the force value at zero. This avoids any tensile stress on the sample and the gap correction (Δh) can be used to calculate the corrected values of the complex modulus:

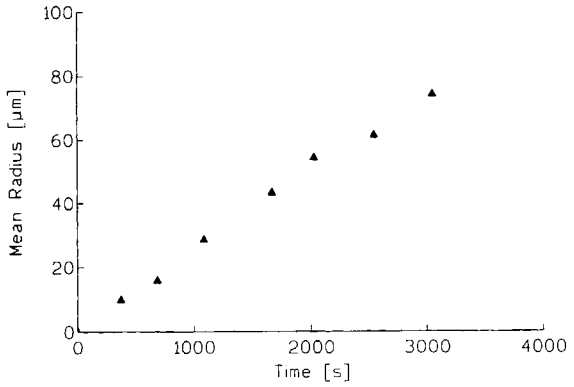

Figure 4 Evolution of the spherulite mean radius during the crystallization at 135°C.

$$\frac{G^*_{\text{real}}}{G^*_{\text{cal}}} = \left(1 - \frac{\Delta h}{h}\right)^{-3} \tag{9}$$

Differential Scanning Calorimetry

Isothermal crystallization was performed in a Perkin–Elmer System-7 differential scanning calorimeter in the same conditions as those used for the rheological measurements. Multiple experiments show an excellent reproducibility of the results.

Polarized Light Microscopy

The characterization of the morphology of the crystalline phase is done in the same conditions as those used for rheometry and calorimetry. It was achieved by means of an optical microscope Leitz Orthoplan equiped with a Mettler heating device. The temperature is accurately controlled.

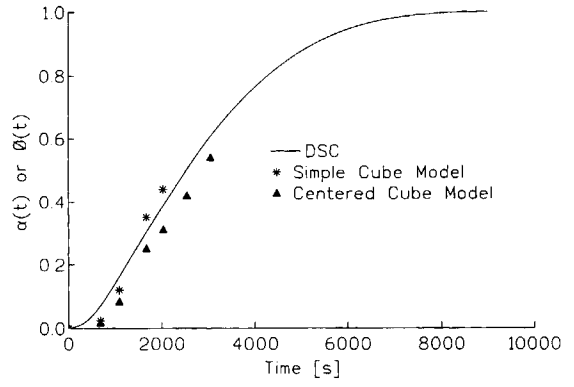

Figure 5 Comparison between the transformed fraction $\alpha(t)$ obtained by DSC and the volume fraction of filler $\phi(t)$ calculated from polarized light microscopy.

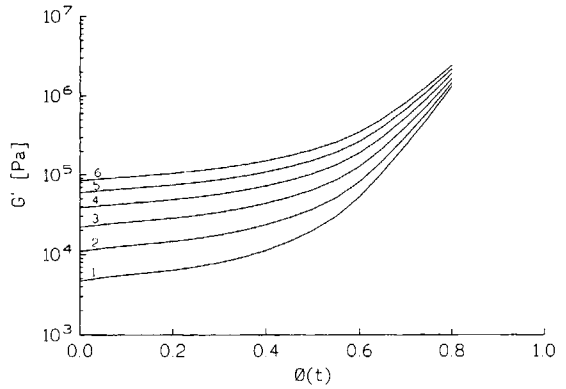

Figure 6 Evolution of the storage modulus with the filler content $\phi(t)$. Frequency: (1) ω = 0.3162 rad/s; (2) ω = 1 rad/s; (3) ω = 3.162 rad/s; (4) ω = 10 rad/s; (5) ω = 31.62 rad/s; (6) ω = 100 rad/s.

RESULTS AND DISCUSSION

Evolution of the Storage and Loss Moduli G' and G'' during Crystallization

Figures 1 and 2 show, respectively, the variation with time of the storage and loss moduli during the crystallization at 135°C for six frequencies. From the two plots, it can be deduced that the moduli are sensitive to the structural changes inside the material during the crystallization. The storage and loss moduli increase with increasing time, and assuming that the time axis is an indication of the filler content, they increase with increasing filler content. Higher moduli are obtained with higher frequencies and at the end of crystallization, i.e., for higher filler content, each modulus tends to reach a unique plateau whatever the frequency. The storage modulus plateau is well distinguished. However, for the loss

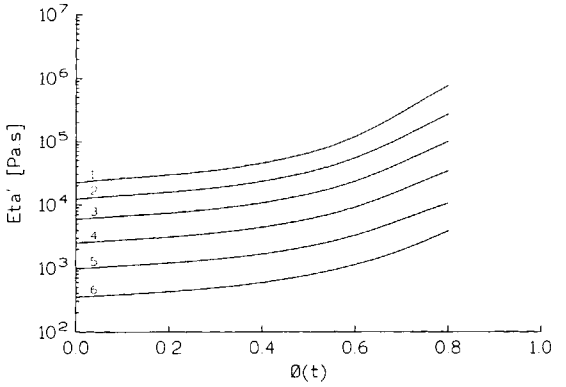

Figure 7 Evolution of the real part of the dynamic viscosity with the filler content $\phi(t)$. Frequency: (1) ω = 0.3162 rad/s; (2) ω = 1 rad/s; (3) ω = 3.162 rad/s; (4) ω = 10 rad/s; (5) ω = 31.62 rad/s; (6) ω = 100 rad/s.

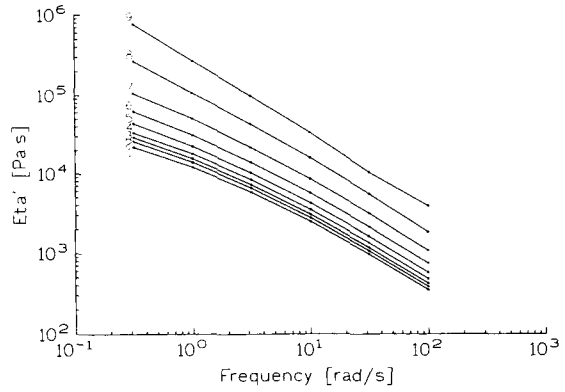

Figure 8 Evolution of the real part of the dynamic viscosity with frequency. Filler content: (1) $\phi = 0$; (2) $\phi = 0.1$; (3) $\phi = 0.2$; (4) $\phi = 0.3$; (5) $\phi = 0.4$; (6) $\phi = 0.5$; (7) $\phi = 0.6$; (8) $\phi = 0.7$; (9) $\phi = 0.8$.

modulus highly dispersed values were observed in the plateau zone. This might be attributed to a possible slippage between the sample and the plate or to a bad resolution for phase measurements when the storage modulus is much greater than the loss modulus (nearly solid material).

Relation between the Transformed Fraction $\alpha(t)$ and the Filler Content $\phi(t)$

The evolution of the transformed fraction $\alpha(t)$ with time is obtained from the endotherm by subsequent integration and normalization. The transformed fraction defines the fraction of polymer transformed into spherulites. The spherulites are considered as filler particles; therefore, it is necessary to establish the relation existing between $\alpha(t)$ and the filler content or fraction of spherulites $\phi(t)$.

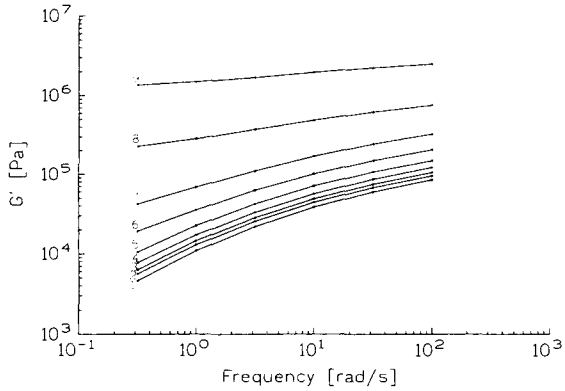

Figure 9 Evolution of the storage modulus with frequency. Filler content: (1) $\phi = 0$; (2) $\phi = 0.1$; (3) $\phi = 0.2$; (4) $\phi = 0.3$; (5) $\phi = 0.4$; (6) $\phi = 0.5$; (7) $\phi = 0.6$; (8) $\phi = 0.7$; (9) $\phi = 0.8$.

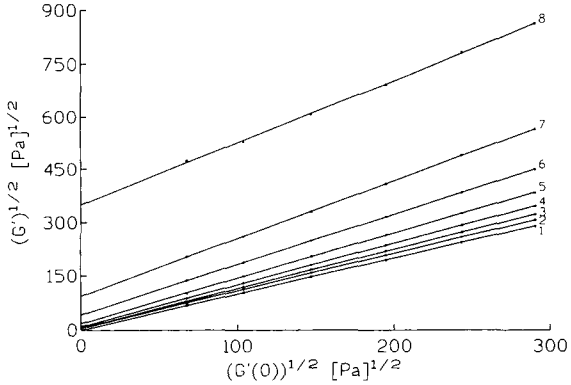

Figure 10 Determination of the yield value of the storage modulus using the modified Casson relation. Filler content: (1) $\phi = 0$; (2) $\phi = 0.1$; (3) $\phi = 0.2$; (4) $\phi = 0.3$; (5) $\phi = 0.4$; (6) $\phi = 0.5$; (7) $\phi = 0.6$; (8) $\phi = 0.7$; (9) $\phi = 0.8$.

At a given time, t, we may assume that the degree of crystallinity $\chi(t)$ is related to the degree of crystallinity inside the spherulite $\chi_s(t)$ by:

$$\chi(t) = \phi(t) \cdot \chi_s(t) \tag{10}$$

To relate $\alpha(t)$ to $\phi(t)$, two approaches were examined. In the first one, we consider that the extraspherulitic crystallization is negligible, and the end of the crystallization process correponds to entities in contact. This approach introduces the concept of the maximum packing volume, thus, at the end of crystallization:

$$\chi_\alpha = \phi_M \cdot \chi_{S\alpha} \tag{11}$$

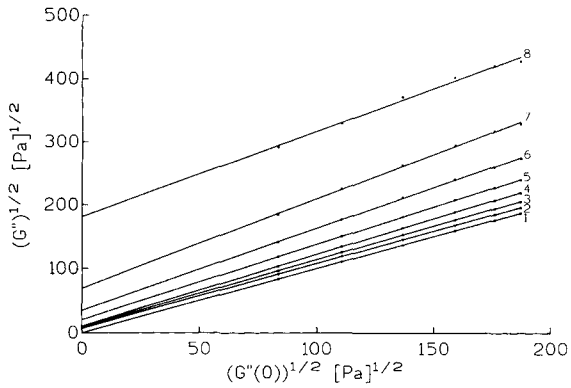

Figure 11 Determination of the yield values of the loss modulus using the modified Casson relation. Filler content: (1) $\phi = 0$; (2) $\phi = 0.1$; (3) $\phi = 0.2$; (4) $\phi = 0.3$; (5) $\phi = 0.4$; (6) $\phi = 0.5$; (7) $\phi = 0.6$; (8) $\phi = 0.7$; (9) $\phi = 0.8$.

Table I Yield-Values of the Storage and the Loss Moduli at Different Filler Contents

$\phi(t)$	G'_y [Pa]	$\frac{G'_y}{G'(0.3162)}$ [%]	G''_y [Pa]	$\frac{G''_y}{G''(0.3162)}$ [%]
0	0	0	0	0
0.1	$2.30\ 10^1$	0.4	$4.50\ 10^1$	0.5
0.2	$3.50\ 10^1$	0.6	$7.30\ 10^1$	0.8
0.3	$9.10\ 10^1$	1.2	$1.00\ 10^2$	0.9
0.4	$3.18\ 10^2$	3.0	$4.00\ 10^2$	2.8
0.5	$1.80\ 10^3$	9.4	$1.20\ 10^3$	6.0
0.6	$8.65\ 10^3$	20.7	$4.80\ 10^3$	14.1
0.7	$1.23\ 10^5$	54.3	$3.28\ 10^4$	38.5
0.8	$1.05\ 10^6$	78.3	$1.60\ 10^5$	65.6

ϕ_M is the maximum packing fraction. It is equal to 0.62 for a random packing of rigid spheres.[19] $\chi_{s\alpha}$ is the final degree of crystallinity inside the spherulite.

Assuming that the degree of crystallinity inside the spherulites is constant during time, therefore:

$$\alpha(t) = \frac{\phi(t)}{\phi_M} \tag{12}$$

The final crystallization rate χ_α was determined by density measurements. It was found to be 61%. Considering the first approach, this value of final degree of crystallinity gives, for random packing of hard spheres, a degree of intraspherulitic crystallinity equal to 100%. This appears to be improbable and, hence, this first approach does not seem to be very suitable. In the second approach, we can envisage an extraspherulitic crystallization during the later times of the isotherm, therefore:

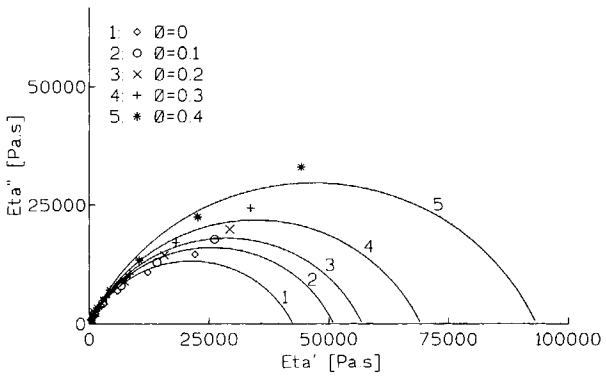

Figure 12 Cole–Cole diagram in absence of the yield effect. Filler content: (1) $\phi = 0$; (2) $\phi = 0.1$; (3) $\phi = 0.2$; (4) $\phi = 0.3$; (5) $\phi = 0.4$.

Table II Parameters of the Cole–Cole diagram at different filler contents

$\phi(t)$	η_0 [Pa·s]	λ_0 [s]	h
0	$4.24\ 10^4$	2.36	0.29
0.1	$5.10\ 10^4$	2.49	0.30
0.2	$5.71\ 10^4$	2.51	0.29
0.3	$6.92\ 10^4$	2.71	0.29
0.4	$9.34\ 10^4$	2.96	0.29

$$\chi_\alpha = \chi_{S\alpha} \tag{13}$$

Thus:

$$\alpha(t) = \frac{\chi(t)}{\chi_\alpha} = \phi(t) \tag{14}$$

Determination of the Spherulites Mean Radius

During the isothermal crystallization, six photographs [Fig. 3(a–f)] have been taken at different time intervals. The time origin was taken at the beginning of the isotherm. From these photographs, and until 11.4 min, it can be noticed that the number of spherulites remains constant, i.e., all the nucleation sites have appeared almost at the same moment. For each time the spherulite mean radius was measured. Figure 4 shows the variation of the mean radius with time. From the beginning of the crystallization, a linear increase of the mean radius of spherulites is observed. It corresponds to the growing step.

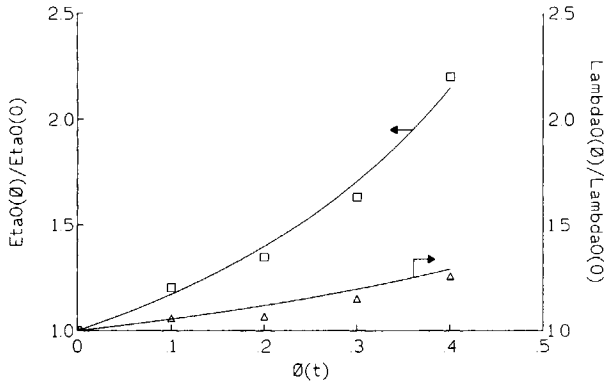

Figure 13 Comparison between experimental (symbols) and model (solid line) relative values of η_0 and λ_0 [Eqs. (22) and (23)].

Table III Error between Experimental and Model Relative Values of η_0 and λ_0 in Absence of Yield Effect

$\phi(t)$	$\frac{\eta_0(\phi)}{\eta_0(0)}$ Exp.	$\frac{\eta_0(\phi)}{\eta_0(0)}$ Model	Relative Error [%]	$\frac{\lambda_0(\phi)}{\lambda_0(0)}$ Exp.	$\frac{\lambda_0(\phi)}{\lambda_0(0)}$ Model	Relative Error [%]
0	1	1	0	1	1	0
0.1	1.20	1.17	−2.5	1.06	1.05	−0.9
0.2	1.35	1.40	+3.7	1.06	1.12	+5.7
0.3	1.63	1.71	+4.9	1.15	1.20	+4.3
0.4	2.20	2.15	−2.3	1.25	1.29	+3.2

Correlation between DSC and Polarized Light Microscopy

The aim is to relate the transformed fraction $\alpha(t)$ or $\phi(t)$ to the relative volume, V_r, calculated using the microscopy results. This relative volume (or filler content) is defined as the volume occupied by the spherulites, at a given time, over the total volume occupied by both spherulites and the matrix liquid. At first, we measured the relative area S_r, defined as the area occupied by spherulites over the total area. As seen in the photographs, the dispersion of the spherulites in the space is a random one. However, to get the relative volume V_r, which corresponds to the filler content, two models of dispersion are proposed: simple cubic, and centered cubic models. These models enable us to estimate the volume fraction from the observed surface fraction.

For the simple cubic model:

$$S_r = \frac{\pi R^2}{a^2} \tag{15}$$

and

$$V_r = \frac{4}{3}\pi\left(\frac{S_r}{\pi}\right)^{3/2} \tag{16}$$

Table IV Error Made between the Experimental and the Predicted Relative Plateau Modulus in Absence of Yield Effect

$\phi(t)$	$\frac{G_0(\phi)}{G_0(0)}$ Exp.	$\frac{G_0(\phi)}{G_0(0)}$ Model	Relative Error [%]
0	1	1	0
0.1	1.12	1.11	−0.9
0.2	1.24	1.25	+0.8
0.3	1.42	1.43	+0.7
0.4	1.75	1.67	−4.5

where R is the spherulite radius and a the width of the cube side.

The maximum spherulite radius that can be obtained is $R_{max} = a/2$; then the maximum relative volume that can be reached is 0.52.

For the centered cubic model:

$$S_r = \frac{2\pi R^2}{a^2} \tag{17}$$

and

$$V_r = \frac{8}{3}\pi\left(\frac{S_r}{2\pi}\right)^{3/2} \tag{18}$$

The maximum relative volume that can be obtained in this case is 0.68. This corresponds to a maximum spherulite radius of

$$\frac{a\sqrt{3}}{4}.$$

Figure 5 shows the results obtained from DSC and microscopy (for both simple cubic and centered

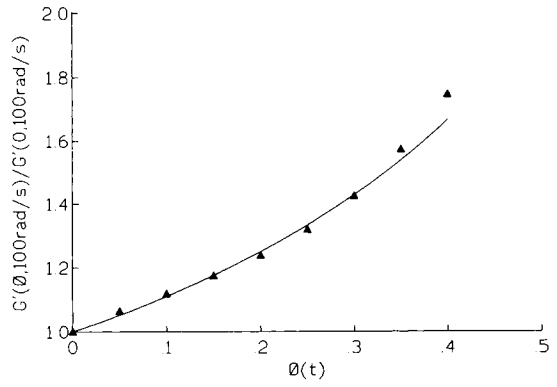

Figure 14 Comparison between the experimental (symbols) and the predicted (solid line) relative values of the plateau modulus.

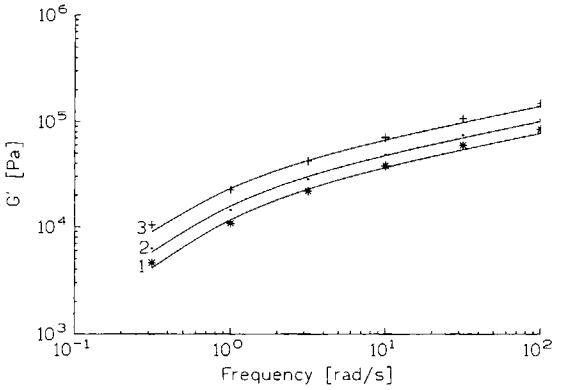

Figure 15 Comparison between the experimental (symbols) and the predicted (solid line)storage modulus. Filler content: (1) $\phi = 0$; (2) $\phi = 0.2$; (3) $\phi = 0.4$.

cubic models). As presented in this figure, the two models do not fit well the results obtained from DSC. However, if we compare the values of the maximum packing volume (0.62 for a random dispersion of spheres, 0.52 for simple cubic, and 0.68 for the centered cubic), it can be clearly seen that the reality is somehow in between the two models. Nevertheless, it can be noticed that these results (DSC and microscopy) tend to confirm the second approach proposed to relate $\alpha(t)$ to $\phi(t)$, which stated that $\alpha(t)$ is equal to $\phi(t)$ rather than the first one.

Influence of the Frequency on the Rheological Functions

Using results of DSC and the rheometry, and for the same time, the evolutions of G' and η' with the filler content $\phi(t)$ for different frequencies are plotted on Figures 6 and 7. It can be noticed that the influence of the frequency on G' is very important at low filler content. Oppositely, at the end of crystallization, the value of the modulus is almost the same whatever the frequency is. This allows us to say that at the end of the crystallization, we tend towards a relatively frozen structure where the mobility is reduced. However, the influence of the frequency on η' is the same during the whole crystallization process. It is worth noticing that the evolution of G'' and η'' is similar to that of G' and η', respectively. This divergence of the rheological functions at higher filler content allows to consider expressions similar to those proposed by different authors:[1-17]

$$\frac{F(\omega, \phi)}{F(\omega, 0)} = g(\phi) \qquad (19)$$

However, it is obvious that this type of expression seems to be only applicable to viscosities. In the case of the moduli, the function of ϕ of the right side of Eq. (19) seems to be also a frequency-dependent term.

Influence of the Filler Content on the Rheological Functions

Figure 8 shows the evolution of η' with the frequency at the different filler contents $\phi(t)$ (flow curves). It can be noticed that, as expected, the incorporation of the filler increases the viscosity compared to that of the liquid matrix ($\phi = 0$). Also, it is found that the increase of the viscosity is very important at low frequencies above a critical value of the filler content. This means that at low frequency the viscosity is very sensitive to structural changes. This phenomenon might be related to a yield effect. The evolution of G' with the frequency at different filler content (Fig. 9) confirms the existence of a yield effect, which can be attributed to an interparticular association leading to a network formation. Indeed, the increase of G' is very important at low frequency and above a critical value of ϕ near 0.4 where an inflexion point is observed. For $\phi \leq 0.6$, the behavior is typically similar to that of a viscoelastic solid. Once again, G'' and η'' show the same evolutions as G' and η', respectively.

Determination of the Yield Values of G' and G''

To determine the yield values of G' and G'' at the different filler content, the modified Casson relation rewritten by Utracki[19] is used:

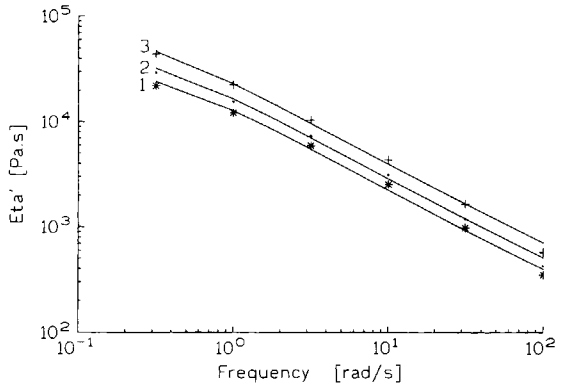

Figure 16 Comparison between the experimental (symbols) and the predicted (solid line) values of the real part of the dynamic viscosity. Filler content: (1) $\phi = 0$; (2) $\phi = 0.2$; (3) $\phi = 0.4$.

$$F^{1/2} = F_y^{1/2} + aF_0^{1/2} \tag{20}$$

where F is the rheological function, F_y indicates the yield value of F, F_0 is the F-value of the pure liquid matrix, and a is a measure of the relative value of F.

The plots of $G'^{1/2}$ and $G''^{1/2}$ vs., respectively, $G'(0)^{1/2}$ and $G''(0)^{1/2}$ give straight lines (Figs. 10 and 11). And by extrapolation, at the different filler contents, the yield values of G' and G'' were deduced.

In Table I, the yield values G'_y and G''_y are presented. If we take into consideration that the error made on the rheometry measurements is about 5%, it can be considered that the values of the yield that represent less than 5% of the modulus in the lowest frequency range are meaningless and, therefore, negligible. A significant value of the yield appears for a value of ϕ between 0.4 and 0.5. This value, though approaching the value of maximum packing fraction $\phi_M = 0.52$ for a simple cube model (taking into account hydrodynamic interactions) remains surprisingly low.

Rheological Behavior in Absence of the Yield Effect ($\phi \leq 0.4$)

In Figure 12 the representation of the viscosity in the complex plane (η'' vs. η') appears to be roughly an arc of a circle for ϕ up to 0.4. This confirms that in this range of volume fraction the behavior of the filled material is mainly that of a viscoelastic liquid. The data were fitted using a mathematical expression of the complex viscosity proposed by Cole and Cole:[32]

$$\eta^*(\omega) = \frac{\eta_0}{1 + (i\omega\lambda_0)^{1-h}} \tag{21}$$

where η_0 is the newtonian viscosity, λ_0 a characteristic time of the model, and h the distribution parameter of the relaxation times. The experimental model parameters are presented in Table II. The study of the model parameters of the Cole–Cole diagram applied to the different curves (ϕ up to 0,4) leads us to postulate the following variations for η_0 and λ_0:

$$\eta_0(\phi) = \eta_0(0)(1 - \phi)^{-3/2} \tag{22}$$

$$\lambda_0(\phi) = \lambda_0(1 - \phi)^{-1/2} \tag{23}$$

It is worth noticing that the distribution parameter h remains constant, which means that there is no modification in the distribution of the relaxation times. In other words, all the times of the spectrum are modified with the same manner according to Eq. (23).

In Figure 13 the evolutions of the experimental (symbols) and model (solid line) relative values of η_0 and λ_0 with the filler content are presented. Table III shows that the errors made between them do not exceed 6%. These results are in contradiction with Leonov's approach,[20] but confirm the approaches of Poslinski et al.[12] and Utracki:[21] the relaxation times of the polymer matrix are dependent on the filler content. Moreover, because all relaxation times are changed in the same manner and using the above results, it can be shown that for the plateau modulus:

$$G_0(\phi) = \frac{\eta_0(\phi)}{\lambda_0(\phi)} = G_0(0)(1 - \phi)^{-1} \tag{24}$$

In Figure 14 and Table IV, the experimental data of the relative plateau modulus taken from data of the relative storage modulus at the highest frequency

$$\frac{G'(\phi, 100 \text{ rad/s})}{G'(0, 100 \text{ rad/s})}$$

are compared to the calculated ones using the above expression. It can be noticed that the model fits well the experimental data because the maximum error made do not exceed 5%.

To ensure that the proposed models allow a good reproduction of the experimental data, the predicted $\eta_0(\phi)$ and $\lambda_0(\phi)$ were used in the Cole–Cole expression and the storage modulus and the dynamic viscosity were calculated. Figures 15 and 16 show a good agreement between the calculated values and the experimental ones. The error made do not exceed 5% (only three filler contents are presented for comprehension purposes).

CONCLUSION

Results obtained from DSC, Polarized Light Microscopy, and Dynamic Rheometry during isothermal crystallization of polypropylene from the melt at 135°C show that such a molten and crystallizing polymers do provide a useful model for filled polymers. The approach that states that the transformed fraction $\alpha(t)$ representing the amount of matter transformed into spherulites is equal to $\phi(t)$ was shown to be the most credible. Variations of the real and the imaginary parts of both the complex viscosity and the complex modulus with the filler content reveal the existence of a yield effect at higher

volume fraction ($\phi > 0.4$). In the absence of this yield effect, the behavior of the material is that of a classical viscoelastic liquid and we proposed a model to predict the variation of the rheological parameters with the volume fraction of filler. These empirical equations show a good agreement with the experimental data. The model equations state that both the plateau modulus or the plateau viscosity and the characteristic times of relaxation depend on the filler content. Moreover, all relaxation times are changed in the same manner and the shape of the relaxation time distribution remains unchanged. This is an interesting result because there are contradictions in the literature about the former point.

Some work is now in progress concerning the higher filler content and the origin of yield value, which seems to be much more related to solid viscoelasticity. Other systems with different crystallizing structures are also under investigation.

REFERENCES

1. I. R. Rutgers, *Rheol. Acta,* **2,** 202 (1962).
2. J. S. Chong, E. B. Christiansen, and A. D. Bayer, *J. Appl. Polym. Sci.,* **15,** 2007 (1971).
3. M. R. Kamal and A. Mutel, *J. Polym. Eng.,* **5,** 293 (1985).
4. N. J. Mills, *J. Appl. Polym. Sci.,* **15,** 2791 (1971).
5. S. Onogi, T. Matsumoto, and Y. Warashina, *Trans. Soc. Rheol.,* **17,** 175 (1973).
6. T. Matsumoto, C. Hitomi, and S. Onogi, *Trans. Soc. Rheol.,* **19,** 541 (1975).
7. T. S. Cantu and J. M. Caruthers, *J. Appl. Polym. Sci.,* **27,** 3079 (1982).
8. R. E. S. Bretas and R. L. Powell, *Rheol. Acta,* **24,** 69 (1985).
9. S. De Rong and C. E. Chaffey, *Rheol. Acta,* **27,** 186 (1988).
10. J. D. Miller, M. Ishida, and F. H. J. Maurer, *Rheol. Acta,* **27,** 397 (1988).
11. D. L. Faulkner and L. R. Schmidt, *Polym. Eng. Sci.,* **17,** 657 (1977).
12. A. J. Poslinski, M. E. Ryan, R. K. Gupta, S. G. Seshadri, and F. J. Frechette, *J. Rheol.,* **32,** 703 (1988).
13. E. H. Kerner, *Proc. Phys. Soc.,* **69B,** 808 (1956).
14. E. H. Takayanagi, S. Minami, and S. Uemara, *J. Polym. Sci.,* **5,** 113 (1964).
15. R. A. Dickie, *J. Appl. Polym. Sci.,* **17,** 45 (1973).
16. R. A. Dickie, M. F. Cheung, and S. Newman, *J. Appl. Polym. Sci.,* **17,** 65 (1973).
17. J. P. Palierne, *Rheol. Acta,* **29,** 204 (1990).
18. N. Casson, *Rheology of Dispersed Systems,* Pergamon Press, London, 1959.
19. L. A. Utracki, in *Rheological Measurement,* A. A. Collyer and D. W. Clegg, Eds., Elsevier Applied Science, London, 1988.
20. A. I. Leonov, *J. Rheol.,* **34,** 1039 (1990).
21. L. A. Utracki, *Rubber Chem. Technol.,* **57,** 507 (1984).
22. C. Carrot, J. Guillet, and K. Boutahar, *Rheol. Acta,* **32,** 566 (1993).
23. J. W. Teh, H. P. Blom, and A. Rudin, *Polymer,* **35,** 1680 (1994).
24. G. Natta and P. Corradini, *Nuevo Cimento Suppl.,* **15,** 9 (1960).
25. D. R. Norton and A. Keller, *Polymer,* **26,** 704 (1985).
26. A. Turner–Jones, J. M. Aizlewood, and D. R. Backett, *Macromol. Chem.,* **75,** 135 (1964).
27. D. R. Morrow, *J. Macromol. Sci.-Phys.,* **(B3)1,** 53 (1969).
28. F. J. Padden and H. D. Keith, *J. Appl. Phys.,* **30,** 1479 (1959).
29. M. O. B. Idrissi, B. Chabert. and J. Guillet, *Macromol. Chem.,* **187,** 2001 (1986).
30. F. Khoury, *J. Res. Nat. Bur.,* **70A,** 29 (1966).
31. A. S. Vaughan and D. C. Basset, in *Comprehensive Polymer Science,* Vol. 2, C. Booth and C. Price, Eds., Pegamon Press, London, 1993.
32. K. S. Cole and R. H. Cole, *J. Chem. Phys.,* **9,** 341 (1941).

Received July 10, 1995
Accepted October 23, 1995